

CONTINUOUS TIME RANDOM WALK APPROACH TO DYNAMIC PERCOLATION

R. HILFER and R. ORBACH

Department of Physics, University of California, Los Angeles, CA 90024, USA

Received 16 September 1988

We present an approximate solution for time (frequency) dependent response under conditions of dynamic percolation which may be related to excitation transfer in some random structures. In particular, we investigate the dynamics of structures where one random component blocks a second (carrier) component. Finite concentrations of the former create a percolation network for the latter. When the blockers are allowed to move in time, the network seen by the carriers changes with time, allowing for long-range transport even if the instantaneous carrier site availability is less than p_c , the critical percolation concentration. A specific example of this situation is electrical transport in sodium β'' -alumina. The carriers are Na^+ ions which can hop on a two-dimensional honeycomb lattice. The blockers are ions of much higher activation energy, such as Ba^{2+} . We study the frequency dependence of the conductivity for such a system. Given a fixed Ba^{2+} hopping rate, $1/\tau$, the Na^+ ions experience a frozen site percolation environment for frequencies $\omega > 1/\tau$. At frequencies $\omega < 1/\tau$, the Na^+ ions experience a dynamic environment which allows long-range transport, even below p_c . A continuous time random walk model combined with an effective medium approximation allows us to arrive at a numerical solution for the frequency-dependent Na^+ conductivity $\sigma(\omega)$ which clearly exhibits the crossover from frozen to dynamic environment.

1. Introduction

A mechanism of considerable importance for energy, mass or charge transfer in solids is hopping transport [1]. Examples include mixed crystals, metal hydrides, doped semiconductors, amorphous and glassy solids, and transition metal oxides. Most often systems exhibit disorder, usually assumed to be frozen, i.e. not time dependent. Here we investigate transport in systems with dynamic disorder. Specifically, we investigate the dynamics of structures where one random component blocks a second (carrier) component. Finite concentrations of the former create a percolation network for the latter. When the blockers are allowed to move in time, the network seen by the carriers changes with time, allowing for long-range transport even if the instantaneous carrier site availability is less than p_c , the critical percolation concentration. As a specific case, we investigate the frequency dependence of the ionic conductivity in superionic solids containing two species of charge carriers. Our results are of a more general nature, and will apply to a large number of situations where ex-

citation transport takes place in a dynamic environment.

More specifically, in this paper we consider β'' -alumina, a superionic conductor, well known for its ability to transport a variety of cations [2]. The conductivity depends upon ion size, crystallinity, impurity content, stoichiometry, electrode material, and frequency. The structure of β'' -alumina is highly anisotropic with ion transport confined to the mirror plane. Mobile ions can hop between the Beavers–Ross (anti-Beavers–Ross) sites forming a two-dimensional honeycomb lattice. We focus on Na^+ - β'' -alumina where each hexagon in the honeycomb lattice is populated with five Na^+ ions. Our interest in this material stems from the fact that the Na^+ ions in Na^+ - β'' -alumina can be readily exchanged with numerous other ions [3,4]. In the present case, two Na^+ ions are substituted by a Ba^{2+} ion. Techniques for controlling substitutional ionic concentrations in β'' -alumina are well developed [5], allowing the study of two-dimensional percolative transport.

Doping of β'' -alumina with two different ionic species (e.g. Na^+ and Ba^{2+}) can be expected to produce interesting dynamical effects. The activation ener-

gies for these two ionic species are approximately [4,6] 0.35 eV for Na^+ and 0.58 eV for Ba^{2+} . At sufficiently low temperatures, only the lighter and smaller Na^+ ions are mobile, while the Ba^{2+} are essentially frozen [4], blocking the Na^+ ions from those sites occupied by Ba^{2+} ions. The sites available for Na^+ ion occupancy thereby form a frozen two-dimensional percolating network on a honeycomb lattice. At higher temperatures, say room temperature, the Ba^{2+} are also mobile, and the network of sites available to the Na^+ ions is no longer frozen. The Na^+ ions, as our "test particles", will experience a dynamic environment because of the slower but finite Ba^{2+} ion motion. This situation will be termed "dynamic site percolation".

Generally we distinguish between three kinds of "particles": walkers (or test particles), blockers, and vacancies. For the particular system we are examining, $\text{Na}^+-\text{Ba}^{2+}-\beta$ -alumina, the blocker (Ba^{2+}) concentration will be denoted by p . From the critical value 0.6962 for site percolation on the hexagonal lattice [7] the critical blocker concentration is here $p_c \approx 0.3038$. At p_c , the requirement of charge neutrality (two Na^+ ions exchange for one Ba^{2+} plus an uncharged vacancy) leads to a Na^+ ionic concentration of $\approx 23\%$, considerably lower than the 83% in pure $\text{Na}^+-\beta$ -alumina. The low sodium concentration has the advantage that Coulomb correlations between the (charged) test particles, and the concomitant intercluster polarization interaction, are minimized. Experiments to measure the conductivity of such systems are currently underway and have served as the motivation for this work [8].

Let us begin by formulating the problem in terms of a master equation, and then go on to present the objectives and outline of our approach. Assuming independent hopping migration for each of the carriers (Na^+), we have

$$\frac{dP(\mathbf{r}, t)}{dt} = \sum_{\mathbf{r}' \in \langle \mathbf{r} \rangle} [w_{\mathbf{r}'\mathbf{r}}(t) P(\mathbf{r}', t) - w_{\mathbf{r}\mathbf{r}'}(t) P(\mathbf{r}, t)], \quad (1.1)$$

where the sum runs over the sites \mathbf{r}' that are nearest neighbours to site \mathbf{r} . Here, $P(\mathbf{r}, t)$ is the probability to find a test particle at site \mathbf{r} at time t , if it started at $\mathbf{r}=0$ at time $t=0$. The transition rates $w_{\mathbf{r}\mathbf{r}'}(t)$ from \mathbf{r} to \mathbf{r}' are now time-dependent random variables, specified as

$$\begin{aligned} w_{\mathbf{r}\mathbf{r}'}(t) &= w && \text{if site } \mathbf{r}' \text{ is vacant at time } t, \\ &= 0 && \text{if } \mathbf{r}' \text{ is occupied by a blocker} \\ &&& (\text{Ba}^{2+}) \text{ at time } t. \end{aligned} \quad (1.2)$$

The stochastic process determining the $w_{\mathbf{r}\mathbf{r}'}(t)$ is the random walk of all blockers (Ba^{2+} ions), restricted by the excluded volume condition that two blockers cannot occupy the same site at the same time.

Our objective is simply stated: we wish to calculate the frequency-dependent ionic conductivity of the test particle for this (dynamic site percolation) problem. We focus on the parameter regime where the concentration $1-p$ of vacancies is bounded away from the percolation threshold, so that the corresponding correlation length is finite. The time scale τ for blocker motion is taken to be much larger than the inverse local hopping rate of the test particles. Other regimes for τ and p will be investigated elsewhere [9]. We shall assume the blockers do not contribute to the conductivity, and that the external field does not influence the motion of the blockers (i.e. the geometry of the dynamic environment is not affected by the time-dependent external field).

We attack the problem by relating the conductivity of the dynamic problem (blocker hopping time, τ , finite) to that of the frozen case (blocker hopping time, τ , infinite). This will be done in two steps. First, we discuss how large-scale cluster rearrangements influence electrical conduction. Second, we include the fluctuations in the geometry experienced locally by the charge carrier. This program will be carried out using a continuous time random walk (CTRW) approach for the dynamic problem, combined with an effective medium approximation (EMA) for the frozen case. Because we shall use the well-known single bond EMA [10,11] for the frozen case, we are solving the dynamic bond percolation problem, though the CTRW approach is in fact more general.

Dynamic bond percolation, consistent with our microscopic model for β -alumina doped with Ba^{2+} , can be defined as follows. A fraction p of bonds on the hexagonal lattice are occupied. These bonds now play the role of blockers: $w_{\mathbf{r}\mathbf{r}'}=0$ if the bond is occupied (see eq. (1.2)). The bonds move by rotating an angle of 120° around either one of their end points (corresponding to the hopping of a Ba^{2+}). Rotations are allowed only if the new bond position is not al-

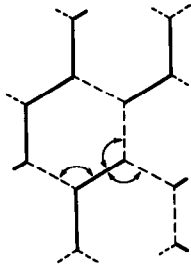


Fig. 1. Example for possible rotations of a single blocking bond around either of its end points when other blockers are present.

ready occupied by another blocking bond (excluded volume condition). Every bond has at most four elementary rotations. Fig. 1 depicts the possible rotations for a single bond if one of the nearest neighbours is occupied by a blocker. It must be emphasized that this model of “dynamic bond percolation” differs from previous models in which renewal processes for either single bonds [12] or full lattice configurations [13] were used to model the dynamics of the environment.

Our main result is a crossover in the frequency-dependent electrical conductivity, $\sigma(\omega)$, from a low-frequency regime dominated by the blocker motion to a high-frequency regime where the carriers experience a frozen disordered environment. The crossover occurs roughly at frequencies $\omega \approx 1/\tau$, where τ is the characteristic time scale for blocker motion. σ remains nearly constant below $1/\tau$, and increases monotonously for higher frequencies. This solution is obtained by incorporating the changing environment as an effective waiting time density for carrier release from finite clusters into the CTRW formulation of the frozen (infinite τ) problem. As a theoretical possibility for other models described by eq. (1.1) we find that the real part of $\sigma(\omega)$ can, for certain release mechanisms, exhibit nonmonotonous behaviour as a function of frequency. Although we do not expect this case for our problem, we have included the results because this possibility is absent [14] for systems described by master equations with time-independent transition rates.

In section 2 we collect the relevant results for continuous time random walks (CTRW) of which we shall make use in later sections. We show in section 3 how rearrangements of vacancy clusters below the percolation threshold can be incorporated into the

waiting time distribution for the CTRW. Using these results, we specify the waiting time distribution in section 4. It will incorporate the release of the test particles from the finite clusters (below an instantaneous percolation threshold) as a consequence of motion of the blockers. Section 5 introduces the effects of fluctuations in the local configurations, thereby completing the specification of the model. The results are presented in section 6. The discussion of section 7 presents a simple physical argument for the crossover in $\sigma(\omega)$, and compares our approach with previous work on the subject.

2. Continuous time random walks

To effect a solution for eqs. (1.1) and (1.2), we must generate a simpler formulation into which the dynamics of the geometry enters only in an averaged manner. The CTRW approach provides such a formulation.

Our first step is to approximate eqs. (1.1) and (1.2) by the generalized master equation,

$$\frac{dP(\mathbf{r}, t)}{dt} = \sum_{\mathbf{r}'(\mathbf{r})} \int_0^t K(\mathbf{r}-\mathbf{r}', t-t') P(\mathbf{r}', t') dt' . \quad (2.1)$$

This constitutes an approximation because we have replaced the time-dependent random transition rates $w_{\mathbf{r}\mathbf{r}'}(t)$ describing the motion of the environment by the nonrandom memory kernel $K(\mathbf{r}, t)$, which describes an average effect of the changing environment.

We now recall that eq. (2.1) is equivalent to the CTRW equation [15],

$$P(\mathbf{r}, t) = \sum_{\mathbf{r}'(\mathbf{r})} \int_0^t \psi(\mathbf{r}-\mathbf{r}', t-t') P(\mathbf{r}', t') dt' + \Phi(t) \delta_{\mathbf{r},0} . \quad (2.2)$$

In this equation, the kernel $\psi(\mathbf{r}, t)$ is the probability density of making a step of vector length \mathbf{r} in a time interval $[t, t+dt]$, and $\Phi(t)$ is the probability for the test particle to remain fixed (i.e. not to jump) for a time t . It is obtained from $\psi(\mathbf{r}, t)$ through

$$\Phi(t) = 1 - \int_0^t \psi(t') dt', \quad (2.3)$$

where $\psi(t)$, called the waiting time distribution, is given by

$$\psi(t) = \sum_r \psi(r, t). \quad (2.4)$$

The CTRW equation, eq. (2.2), has two advantages over the generalized master equation, eq. (2.1). One is that it no longer contains derivatives, but its principal advantage is that it only involves probabilistic quantities. Hence, probabilistic arguments can be used to obtain the kernel ψ for a given problem.

We proceed to relate the frequency-dependent conductivity $\sigma(\omega)$ to the waiting time distribution. The conductivity can be calculated from the Laplace transform of the autocorrelation function $P(r, t)$ via a generalized Einstein relation [10],

$$\sigma(\omega) = \frac{\rho e^2 \hat{D}(\omega)}{k_B T}. \quad (2.5)$$

Here, ρ is the number density of carriers, e the electronic charge, T the absolute temperature and k_B the Boltzmann constant. The frequency-dependent generalized diffusion coefficient $\hat{D}(\omega)$ is given by [10]

$$\hat{D}(\omega) = -\frac{\omega^2}{z} \sum_r r^2 P(r, i\omega), \quad (2.6)$$

where z is the coordination number of the lattice. $P(r, i\omega)$ denotes the Laplace transform $P(r, u)$ of $P(r, t)$ evaluated at $u=i\omega$. We shall use u and $i\omega$ interchangeably.

For dynamic percolation all sites of the underlying regular (here, honeycomb) lattice are in principle accessible to the walkers because the disorder is time dependent. Thus, similar to regular random walk, there is no dependence on the starting point.

We assume the usual decoupling of space and time in the waiting time distribution [11]: $\psi(r, t) = w(r)\psi(t)$. This is justified for hopping models on regular lattices [16,17]^{#1} and is commonly used also for disordered systems. One obtains

^{#1} See, however, ref. [16] for a discussion of the decoupling approximation.

$$D(\omega) = \frac{z}{\langle r^2 \rangle} \hat{D}(\omega) = \frac{i\omega \psi(i\omega)}{1 - \psi(i\omega)}, \quad (2.7)$$

where $\langle r^2 \rangle = \sum r^2 w(r)$, and $D(\omega)$ is a normalized diffusion coefficient. With the use of eq. (2.7), $\sigma(\omega)$ can be calculated from the waiting time distribution $\psi(u)$, the Laplace transform of $\psi(t)$. Note however, that $D(\omega)$ as defined above is in general not equivalent to the Laplace transform of $d\langle R^2(t) \rangle / dt$ [18].

Before concluding this section we remark that the generalized diffusion coefficient D corresponds to the memory kernel in the generalized master equation. It depends on frequency alone because of the decoupling approximation. The inverse Laplace transform of D can be interpreted as an effective time-dependent transition rate for the master equation of a self-consistently determined effective medium.

We now formulate our model as a continuous time random walk.

3. General form of $\psi(t)$

We show in this section how the waiting time distribution for the frozen percolation problem (frozen blockers) below the percolation threshold for vacancies suggests a general form for the waiting time distribution for the dynamic problem. The dynamic site or bond percolation problems described in the introduction will guide the discussion.

We begin with the discussion of the waiting time distribution for the frozen problem. It is shown in the CTRW formalism that [17,11],

$$\langle R^2(u) \rangle \propto \frac{\psi(u)}{u[1 - \psi(u)]}, \quad (3.1)$$

where $\langle R^2(u) \rangle$ denotes the Laplace transform of the mean-square displacement of the random walk. Using eq. (2.7) it follows that

$$\langle R^2(u) \rangle \propto \frac{D(u)}{u^2}. \quad (3.2)$$

The long-time limit of $\langle R^2(t) \rangle$ can be determined from the small u behaviour of $D(u)$. In particular, we note that, if $D(u) \propto c_0$ for $u \rightarrow 0$, one has $\langle R^2(t) \rangle \propto t$, i.e. ordinary diffusive transport. This case obtains for $p > p_c$ in a frozen percolation problem. For $p < p_c$ one must have $D(u) \propto c_1 u$ in order to obtain localization

within finite clusters, i.e. $\langle R^2(t) \rangle \propto \text{const}$. The case $p = p_c$, leading to anomalous behaviour (fractional power laws), is here of minor interest.

Consider now the question how the difference above and below p_c is reflected in the waiting time distribution, $\psi(t)$. To answer this question, one must express ψ in terms of D . Inverting eq. (2.7), we have

$$\psi(u) = \frac{D(u)}{u + D(u)}. \quad (3.3)$$

Writing $D(u) = c_0 + c_1 u + \dots$ above p_c , and $D(u) = c_1 u + \dots$ below, one finds that

$$\int_0^t \psi(t) dt = \lim_{u \rightarrow 0} \psi(u) = 1 \quad \text{for } p > p_c, \\ = \frac{c_1}{1 + c_1} \quad \text{for } p < p_c. \quad (3.4)$$

It can be seen immediately that the waiting time distribution is not normalized below p_c . It lacks the weight $1/(1 + c_1)$. This implies that at every step the random walker has the finite probability $1/(1 + c_1)$ to get trapped forever. Stated differently, the correct normalized waiting time distribution below p_c must be augmented by a δ function at infinity with weight $1/(1 + c_1)$. This finite weight for infinite waiting times produces a constant mean-square displacement in the long-time limit.

We now return to the original dynamic percolation problem with mobile blockers. We will distinguish notationally between the frozen and the dynamic problem using an index 0 for the frozen case. In the following it will be important to remember that waiting time densities and other quantities of the CTRW formulation do not refer to the original dynamic percolation problem, but to an effective random walk on a regular lattice having the same averaged behaviour as the original problem. We will try to use crude physical and probabilistic arguments to arrive at an ansatz for the waiting time density of this effective CTRW.

The basic idea of our approach is suggested by the different structure of the frozen waiting time density $\psi_0(t)$ above and below the percolation threshold p_c . Below p_c , $1 - p < p_c$, one has an immediate starting point because the blockers are mobile and therefore infinite waiting times have zero weight. No such

starting point exists above the percolation threshold, $1 - p > p_c$. Using the freedom introduced by the missing weight below p_c , the waiting time density for the full problem $\psi(t)$ can be decomposed as

$$\psi(t) = a\psi_e(t) + (1 - a)\psi_0(t). \quad (3.5)$$

Here, $\psi_0(t)$ is the density for the frozen problem, while $\psi_e(t)$ is an effective waiting time density which corresponds to an escape from finite clusters. It replaces the δ -function density at infinity for the frozen case. The coefficient a is the probability that the walker in the effective CTRW for the frozen problem would wait an infinite amount of time for its next step, corresponding to a full exploration of all finite clusters. On the other hand, the CTRW evolves as it would in the frozen environment with probability $1 - a$. Eq. (3.5) states that the length of the waiting time between two hops is determined from either $\psi_e(t)$ or $\psi_0(t)$ with probability a or $1 - a$, respectively. Because ψ_e generalizes the infinite waiting time for release from the finite clusters in the frozen problem, we know from the discussion following eq. (3.4) that this occurs with probability

$$a = 1/(1 + c_1), \quad (3.6)$$

which determines a . It is important to realize that the simple decomposition of eq. (3.5) is fundamentally limited to the case $1 - p < p_c$. As $1 - p$ approaches p_c , the coefficient c_1 diverges and the weight a goes to zero. For $1 - p > p_c$ the weight a vanishes because the waiting time distribution is already normalized, as seen in eq. (3.4). Thus, one has $\psi(t) = \psi_0(t)$ for $1 - p > p_c$. This implies that utilizing the missing weight below p_c is not fully sufficient for a satisfactory treatment of the dynamic percolation problem. The new density $\psi_e(t)$ describes only the release from fully explored clusters. The actual hopping attempts of the walker are governed by $\psi_0(t)$ describing a frozen environment. This problem will be taken up in section 5. Here we continue with the specification of $\psi_e(t)$.

To obtain a general form for $\psi_e(t)$ for $1 - p < p_c$ we must distinguish between waiting times between hopping attempts and waiting times caused by being blocked after full exploration of finite clusters. The waiting time between hopping attempts is governed by $\psi_0(t)$. According to eq. (3.5), the walker will be blocked with probability a . During the random

blocking time, however, the walker continues to make jump attempts which remain unsuccessful until geometrical (blocker) rearrangements allow it to move again. The blocked periods are distributed according to a density $\psi_1(t)$ which reflects the dynamics of the rearranging clusters. The instant at which the blocking condition is removed will in general not coincide with a hopping attempt. The random time between the end of the blocked interval and the next jump attempt is called residual waiting time, and is governed by a density $\psi_0^{\text{res}}(t)$. Summing the random blocking time and the residual waiting time gives the random waiting time governed by $\psi_e(t)$. Thus

$$\psi_e(t) = \psi_1(t) * \psi_0^{\text{res}}(t), \quad (3.7)$$

where $*$ denotes the convolution product $f * g = \int_0^t f(t-t')g(t') dt'$ for the density of the sum of two independent random variables with densities f and g . The complete waiting time density has the general form

$$\psi(t) = a\psi_1(t) * \psi_0^{\text{res}}(t) + (1-a)\psi_0(t). \quad (3.8)$$

Before proceeding with the specification of the different densities, we emphasize the difference between ψ_1 and the two other densities. Contrary to ψ_0 and ψ_0^{res} , ψ_1 is itself not a property of the walkers. Rather it describes the dynamics of the finite clusters via the distribution of time intervals during which the walker is blocked. Contrary to the frozen case where each walk is terminated on the average after $1/(1-a)$ steps, the walker is now released after a finite time governed by $\psi_1(t)$.

4. Specification of $\psi(t)$

Section 3 has introduced a general decomposition of the waiting time distribution $\psi(t)$ into $\psi_0(t)$, $\psi_0^{\text{res}}(t)$, and $\psi_1(t)$. These components will be specified in this section. As a result our approach will emphasize the difference between the regime below p_c , described in this section where transport is limited by geometrical rearrangement; and the regime above p_c , described in section 5, where transport is limited by the hops of the test particle.

We discuss first the densities ψ_0 and ψ_0^{res} . The density ψ_0 is obtained from the generalized diffusion coefficient D_0 for the frozen problem which is as-

sumed to be known. Eqs. (3.3) and (3.4) then yield

$$\psi_0(t) = \frac{1+c_1}{c_1} \mathcal{L}^{-1} \left(\frac{D_0(u)}{u+D_0(u)} \right), \quad (4.1)$$

where \mathcal{L}^{-1} denotes the inverse Laplace transform.

The distribution $\psi_0^{\text{res}}(t)$ is known in the CTRW literature as the waiting time distribution for the first jump [19]. Assuming that the hopping attempts described by ψ_0 have reached a stationary state, one obtains $\psi_0^{\text{res}}(t)$ by averaging ψ_0 over all time spans between the end of the blocking period and the last jump attempt. One finds [19]

$$\begin{aligned} \psi_0^{\text{res}}(t) &= \int_0^\infty \psi_0(t+t') dt' \\ &\times \left(\int_0^\infty \int_0^\infty \psi_0(t+t') dt dt' \right)^{-1}, \end{aligned} \quad (4.2)$$

where the denominator is a normalization factor. Comparison with eq. (2.3) leads to

$$\psi_0^{\text{res}}(t) = \Phi_0(t) \left(\int_0^\infty \Phi_0(t) dt \right)^{-1} = \Phi_0(t) / \bar{t}_0, \quad (4.3)$$

where

$$\begin{aligned} &\int_0^\infty \Phi_0(t) dt \\ &= \lim_{u \rightarrow 0} \Phi_0(u) = \lim_{u \rightarrow 0} \left(- \frac{d\psi_0(u)}{du} \right) = \bar{t}_0 \end{aligned} \quad (4.4)$$

is the average of the frozen density $\psi_0(t)$.

Finally we turn to the determination of $\psi_1(t)$. It is the central new ingredient in our approach. ψ_1 reflects the effect of rearrangements necessary to release a blocked random walker. In order to obtain an expression for ψ_1 it is helpful to consider the case where the concentration of vacancies is low, i.e. $p \approx 1$. In this case the walker is blocked most of its time. The length of a blocked interval is the time between two consecutive visits of a vacancy to any of the nearest neighbour sites of the blocked walker. Because we consider only hard-core repulsions between blockers the vacancies can move independently of each other, and their trajectories are realizations of a Markov

process. Therefore, at any given instant, the residual blocking time depends only on the present configuration. It is unaffected by the past, and has the same distribution as the blocking time itself. This “lack of memory” implies that the blocking times are exponentially distributed [20], and thus

$$\psi_1(t) = \tau_1^{-1} e^{-t/\tau_1}. \quad (4.5)$$

The average blocking time τ_1 is related to the density $1-p$ of vacancies and their hopping time τ by

$$\tau_1 = \tau / (1-p), \quad (4.6)$$

because each site is occupied once every $1/(1-p)$ steps in units of τ . This argument breaks down if there are spatial or temporal correlations between vacancies coming for example from long range interactions.

We digress for a moment to describe a possible form of ψ_1 that might arise for other models because it leads to interesting theoretical consequences. Suppose that the release mechanism described by ψ_1 is sequential. This means the length of a blocking interval is made up from a number of shorter intervals of random length. These shorter intervals represent a sequence of substeps necessary to release the walker. The total blocking time is the sum of the times for all substeps. Then the central limit theorem will lead to a Gaussian distribution for ψ_1 if the number of necessary substeps becomes large. The main difference with (4.5) is that ψ_1 would no longer be monotonically decreasing. In order to study this possibility we have considered the case that there are an average of n identically distributed substeps following an exponential distribution with mean τ_2 . This leads to a density

$$\psi_1'(t) = \frac{1}{\tau_2} \left(\frac{t}{\tau_2} \right)^{n-1} \frac{1}{\Gamma(n)} e^{-t/\tau_2}, \quad (4.7)$$

where $\Gamma(n)$ denotes the gamma function. We use this formula also for noninteger n in the sense of an interpolation between integer values. Note that for $\tau_2 = \tau_1$ and $n = 1$ eq. (4.7) becomes eq. (4.5).

This concludes the discussion of the waiting time distribution.

5. Configuration renewal

We have been concerned up to now with the effects of release from finite clusters below the percolation

threshold ($1-p < p_c$). We now return to the full range of blocker concentrations p , and include the averaged effect of fluctuations in the geometry experienced by the test particle at every step.

The waiting time density $\psi(t)$, specified in section 4, treats the individual hopping instants of the test particle as being given by $\psi_0(t)$. If not blocked, the walker behaves in the same way as in the frozen percolation problem. Such a description is clearly unsatisfactory because it neglects the changes in the local environment experienced by the particle at every step. This will be taken into account by renewing the configuration after a typical renewal time τ_r . If the renewal time τ_r is chosen long enough so that the memory of the last configuration has been lost, one is led to an exponential renewal process with density

$$\psi_r(t) = \tau_r^{-1} e^{-t/\tau_r} \quad (5.1)$$

for the random time intervals between subsequent renewals. Thus, instead of following the trajectory of every blocker, we update the entire lattice configuration. The average time τ_r between updates is chosen such that the memory of the configuration after the last renewal has been completely lost.

To specify the renewal time τ_r , we distinguish between $1-p < p_c$ and $1-p \geq p_c$. In the former case, the configuration of vacancies constitutes the disordered environment for the test particles by means of a deviation from the completely blocked situation at $p = 1$. In the latter case, the configuration of blockers forms a deviation from the vacant lattice, $p = 0$. The criterion for memory loss of the last configuration is that the diffusing quantities (blockers or vacancies) must diffuse at least the average distance between them. For blockers the average distance is $p^{-1/d}$, for vacancies $(1-p)^{-1/d}$. The average number of steps necessary to diffuse this distance is therefore proportional to $p^{-2/d}$ for blockers, and $(1-p)^{-2/d}$ for vacancies. Assuming, as before, that the individual steps of blockers or vacancies occur with the typical hopping time τ of the blockers, leads to a renewal time

$$\begin{aligned} \tau_r &= \left(\frac{p_c}{1-p} \right)^{2/d} \tau \quad \text{for } 1-p < p_c, \\ &= \left(\frac{1-p_c}{p} \right)^{2/d} \tau \quad \text{for } 1-p \geq p_c, \end{aligned} \quad (5.2)$$

where we have chosen the normalization so that $\tau_r = \tau$

for $1-p=p_c$, i.e. at p_c the memory is already lost if each blocker (or vacancy) moves once.

The effect of an exponential renewal process on the generalized diffusion coefficient for the frozen problem has been analyzed in previous work [13]. It was found that the diffusion coefficient for the system with configuration renewal is given as $D_0(u+1/\tau_r)$ where $D_0(u)$ is the generalized diffusion coefficient for the frozen problem. Incidentally, the same result was obtained from an effective medium approximation for a system where single bonds are renewed individually at a rate τ_r [12]. The result can be understood from the remark in section 2 that the inverse Laplace transform of the generalized diffusion coefficient can be interpreted as a generalized time-dependent effective transition rate in a master equation. The transition rate for the frozen problem can only be used for a time interval during which no renewal occurs. Because the renewal process is assumed to be independent of the jump process, one has to multiply the transition rates by the probability ϕ_r of no renewal during the given time interval. Hence,

$$D(t) = D_0(t) \phi_r(t), \quad (5.3a)$$

where

$$\phi_r(t) = 1 - \int_0^t \psi_r(t') dt' = e^{-t/\tau_r}. \quad (5.3b)$$

One obtains the desired result by taking the Laplace transform of this equation.

This result can be applied directly to the generalized diffusion coefficient resulting from the waiting time distribution $\psi(t)$ specified in sections 3 and 4. In this way we use configuration renewals to account for the fluctuations in the geometry seen by the walker at every step. This constitutes a severe approximation because it neglects the correlations in the time development of the geometry. We have kept some effects from those correlations by using the freedom of the missing weight to modify the waiting time distribution and have introduced a concentration-dependent renewal rate.

6. Results for the hexagonal lattice

Before actually solving our model for the case of interest, the two-dimensional honeycomb lattice, we

collect all formulas in their Laplace-transformed version.

First, we determine the Laplace transform $\psi(u)$ of $\psi(t)$. From the discussion in section 3, we recall that $D_0(u) \propto c_1 u$ for small u . Here, and in the following, we set the time scale for the hopping of the walkers (test particles) to unity. Then, to second order in u , we can write

$$D_0(u) = c_1 u + c_2 u^2 + O(u^3), \quad (6.1)$$

for $1-p < p_c$. Further, for the Laplace transform of the density of blocking periods, we find from eqs. (4.5) and (4.6),

$$\psi_1(u) = \left(1 + \frac{u\tau}{1-p}\right)^{-1}. \quad (6.2a)$$

Transformation of eq. (2.3), using eq. (4.3), yields

$$\psi_0^{\text{res}}(u) = \frac{1 - \psi_0(u)}{u\bar{t}_0}. \quad (6.2b)$$

\bar{t}_0 can be determined using eqs. (4.4) and (6.1) to give

$$\bar{t}_0 = -\frac{c_2}{c_1(1+c_1)}. \quad (6.2c)$$

We now obtain $\psi(u)$ by transformation of eq. (3.8),

$$\begin{aligned} \psi(u) &= \left(1 + \frac{u\tau}{1-p}\right)^{-1} \frac{D_0(u) - c_1 u}{c_2 u [u + D_0(u)]} \\ &\quad + \frac{D_0(u)}{u + D_0(u)}, \end{aligned} \quad (6.2d)$$

where eqs. (3.6), (4.1) and (6.2a)–(6.2c) have been employed. Eq. (6.2d) is to be inserted into eq. (2.7), which itself reads

$$\tilde{D}(u) = \frac{u\psi(u)}{1-\psi(u)}. \quad (6.2e)$$

Finally, we obtain the generalized diffusion coefficient from section 5 as

$$D(u) = \hat{D}(u+1/\tau_r), \quad (6.2f)$$

where τ_r is given by eq. (5.2). Eqs. (6.1), (6.2) and (5.2) collectively represent the formulation of our model. They relate the conductivity of the dynamic percolation model to that of the frozen problem. The only parameters are p , the density of blockers, and $1/$

τ , their relative hopping rate. Both can be fixed in the experiment.

We first calculate the frozen diffusion coefficient $D_0(u)$. This can be performed using standard EMA methods [10,11]. The EMA equation for bond percolation can be rewritten as

$$D_0(u) = \frac{q-p_c - F(u, D_0)}{2(1-p_c)} \times \left[1 \pm \left(1 + \frac{4(1-p_c) F(u, D_0)}{[F(u, D_0) - q + p_c]^2} \right)^{1/2} \right], \quad (6.3a)$$

where $q = 1 - p$ is the vacancy concentration, $p_c = 2/3$, and

$$F(u, D_0) = p_c u G[u/D_0(u)]. \quad (6.3b)$$

Here, $G(x)$ is the Green function at the origin for the hexagonal lattice. It can be expressed in terms of $K(m)$,

$$K(m) = \int_0^{\pi/2} (1 - m \sin^2 \phi)^{-1/2} d\phi, \quad (6.3c)$$

the complete elliptic integral of the second kind, as [11]

$$G(x) = - \frac{2(3+x)}{\pi(2+x)^{3/2}(6+x)^{1/2}} \times K\left(\frac{16(x+3)}{(x+2)^3(x+6)}\right). \quad (6.3d)$$

Taking the limit $u \rightarrow 0$ for the + sign in eq. (6.3a) recovers the well-known dc behaviour: $D(0) = (q - p_c)/(1 - p_c)$ above p_c , while the - sign is used below the percolation threshold. We solve eq. (6.3) for the - sign by an iterative method. The iteration is terminated if the maximal relative change between two consecutive solutions falls below 10^{-13} .

While, in principle, we could obtain c_1 and c_2 from the solution of eq. (6.3), we calculate them independently. It is well known [10,11] that c_1 obeys the equation

$$G(1/c_1)/c_1 = 1 - q/p_c. \quad (6.4a)$$

This equation is solved with the same accuracy as eq. (6.3). c_2 is then obtained from c_1 by expanding $D_0(u)$ around $u = 0$ giving [11]

$$c_2 = - \frac{c_1^3(1-q)}{p_c[G(1/c_1) + G'(1/c_1)/c_1]}, \quad (6.4b)$$

where $G'(1/c_1)$ denotes the derivative of $G(x)$ at $x = 1/c_1$.

The results of a numerical solution are displayed in fig. 2 for $\tau = 5000$ (recall that the typical hopping time for the test particles, Na^+ , has been set equal to unity). This is roughly the value of τ in an experiment at room temperature [4]. Five curves for concentrations below the percolation threshold for the vacancies, $0.4 \leq p \leq 0.6$, are shown. In fig. 3 the same data are plotted logarithmically. In the real part of D one finds a crossover from a regime $\omega < 1/\tau$ controlled by the slow rearrangements of the geometry to the regime $\omega > 1/\tau$ governed by diffusion on finite clusters. The position of the crossover regime shifts to higher frequencies with increasing blocker concentration.

In fig. 4 we plot the dc conductivity on a logarithmic scale as a function of the blocker concentration, p , for various values of τ . The broken line is the effective medium result for frozen percolation ($\tau = \infty$) with a sharp transition at $p = 1/3$. Clearly, the transition is smeared out in the dynamic case. From the nonanalyticity of the function $\tau_c(p)$ at p_c in eq. (5.2), one expects to see some structure. Some structure is present around p_c , becoming more pronounced for smaller τ . However, it is an artifact of the crude mean field type approximations used throughout this paper, and will be absent in more satisfactory treatments.

The same calculations have been performed using ψ'_1 from the sequential release mechanism. One then has from eq. (4.7)

$$\psi'_1(u) = (1 + u\tau_2)^{-n} \quad (6.2a')$$

instead of eq. (6.2a), and eq. (6.2d) has to be modified accordingly. The results are displayed in fig. 5. For comparison we have chosen $\tau_2 = 5000$, and the values $n = 40/36, 40/33, 40/30, 40/27$, and $40/24$. For values of n above $40/36$ the real part of $D(\omega)$ begins to develop a minimum. This can be concluded also from an expansion of eqs. (6.2a')–(6.2e), around $\omega = 0$. We find that $\text{Re } \tilde{D}(\omega)$ decreases for large enough τ_2 . More precisely [9] the curvature for

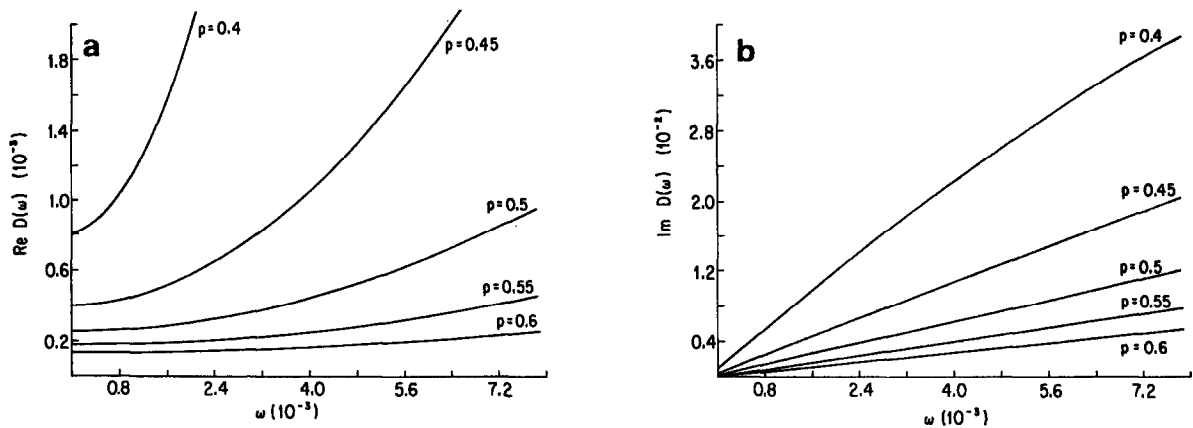


Fig. 2. (a) Real part, and (b) imaginary part of the conductivity as a function of frequency and blocker concentrations. Results for blocker concentrations $p=0.4, 0.45, 0.5, 0.55,$ and 0.6 (from top to bottom) are shown. The hopping time for the blockers is $\tau=5000$, the hopping time for the test particles is unity.

the real part is found to be negative, and proportional to $-\tau_2(c_1+1)(n-1)/n$ in the $\tau_2 \rightarrow \infty$ limit. The dc value, $\text{Re } \tilde{D}(0)$, is given by $c_2(c_1+1)/(\tau_2 n c_2 - c_3)$. Note that it depends upon the third-order coefficient c_3 . Because of the shift implied by eq. (6.2e), this analysis can at best be used in the limit $p \rightarrow 1$ of high blocker concentration. It suggests that the frequency-dependent conductivity, $\sigma(\omega)$, proportional to $D(\omega)$, decreases initially from its dc value as ω increases from zero. Mathematically the resulting minimum in $\sigma(\omega)$ originates from the nonmonotonicity of $\psi'_1(t)$ which results from the sequential nature of the release mechanism. The depth of the minimum in-

creases not only with n but also with τ_2 . This is shown in fig. 6 where the top curve of fig. 5a with $n=40/36$ is plotted for a higher value of $\tau_2=5 \times 10^7$. Note that besides its increase in depth the position of the minimum is shifted to higher values in units of $1/\tau_2$.

7. Discussion and conclusion

The crossover behaviour of $\sigma(\omega)$, exhibited in section 6, can be understood from the following simple argument for Ba^{2+} substitution in $\text{Na}^+-\beta''$ -alumina. At sufficiently low temperatures, say liquid nitrogen

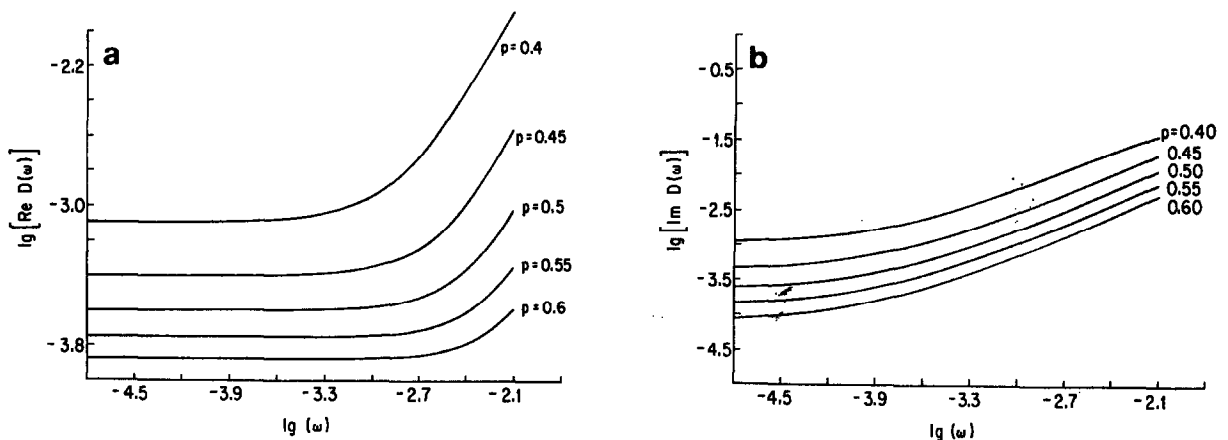


Fig. 3. Same as fig. 2 in a logarithmic plot.

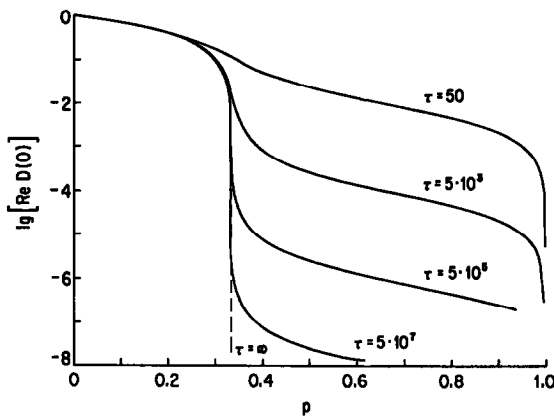


Fig. 4. dc conductivity as a function of blocker density p for hopping time ratios $\tau=5 \times 10^7, 5 \times 10^5, 5 \times 10^3, 50$. The broken line represents the EMA result of frozen percolation with $\tau=\infty$.

temperature, and for high enough blocker (Ba^{2+}) concentrations, p ($1-p$ below the percolation threshold), the dc conductivity must vanish. Warming to room temperature, the Ba^{2+} become mobile, and the sodium ions can get through the network. Hence, $\sigma(0) \neq 0$. Imagine now that the frequency ω is increased from zero. For the moment, take $\omega \geq 1/\tau$. Then, on that time scale, the Ba^{2+} appear frozen. That is, the system appears below the critical threshold p_c for available sites. On the timescale $1/\omega$, the Na^+ will diffuse distances $l(\omega)$ which can be greater than or less than the correlation length, ξ , de-

pending upon temperature and frequency ω . The distance l can be thought of as the square root of the mean-square displacement, eq. (3.2). Consider two cases:

(1) $l(1/\tau) > \xi$. Here, the Na^+ ions will feel the boundaries of all the finite clusters and the conductivity will have essentially its dc value. As ω increases beyond $1/\tau$, $l(\omega)$ will diminish. Eventually, $l(\omega)$ will become less than ξ , and $\sigma(\omega)$ will begin increasing with increasing ω . Thus there should be a crossover in the conductivity in the vicinity of $\omega \approx 1/\tau$.

(2) $l(1/\tau) < \xi$. Here, some of the Na^+ ions will not feel the boundaries of all the finite clusters as ω increases from zero towards $1/\tau$. The conductivity may then increase without a significant change of its behaviour at $1/\tau$.

This simple argument highlights the importance of the interconnected length and time scales in the problem. Our CTRW formulation has, naturally, focused on the time domain. A more direct approach would be to simulate the model. Preliminary results from such simulations seem to support our model calculations [9].

The conductivity minimum resulting from a sequential release mechanism does not occur in hopping models based on a master equation with time-independent transition rates [14]. In this paper, however, we have started from the more general equation (1.1) which includes such an effect as an interesting theoretical possibility. Although this pos-

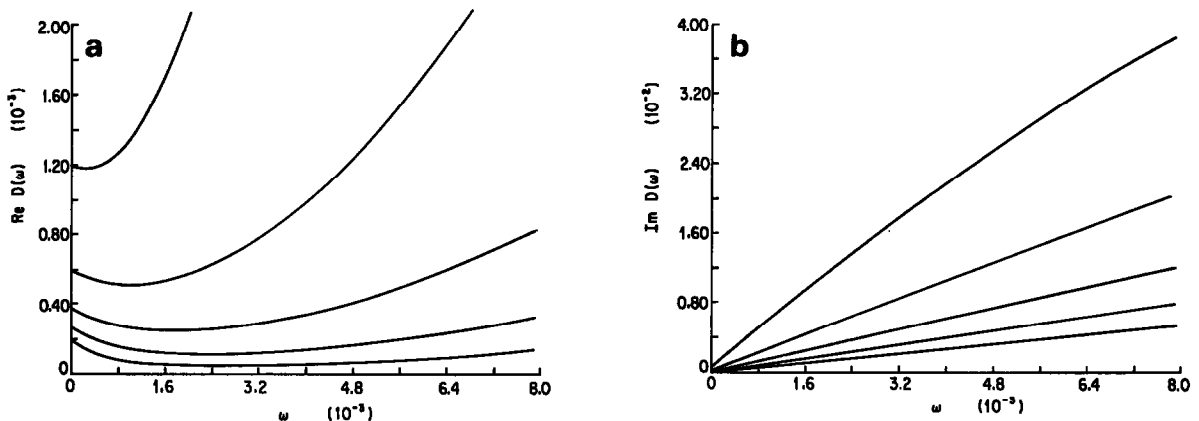


Fig. 5. (a) Real part, and (b) imaginary part of the conductivity using ψ'_1 for the sequential release model from eq. (4.7). Curves for $\tau_2=5000$, and values $n=40/36, 40/33, 40/30, 40/27$ and $40/24$ (from top to bottom) are shown.

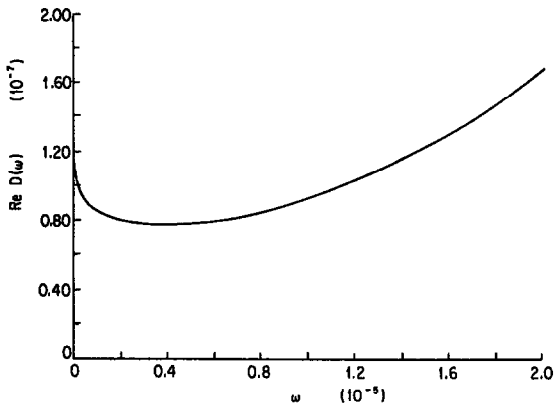


Fig. 6. Real part of conductivity using ψ'_1 for the sequential release model from eq. (4.7) for $n=40/36$ and $\tau_2=5 \times 10^7$.

sibility does not apply to our model it is important to elucidate the physical meaning of a nonmonotonous waiting time density if we wish to understand in which cases it may be relevant. A nonmonotonous waiting time density with a single peak means that the walker jumps according to a badly synchronized clock. Such a situation is therefore intermediate between a discrete time random walk and a continuous time random walk. The conductivity minimum is thus seen to be a resonance effect. A resonance occurs when the frequency of the external field is a multiple of the clock frequency. Consequently one expects to find even more pronounced effects if the clock period becomes more accurate, i.e. if the peak width becomes small. This is indeed observed for the sequential release mechanism if the number of substeps, n , is increased, and will be discussed elsewhere [9].

We conclude the discussion by comparing our approach to previous work that has considered the frequency dependent conductivity [12,13]. The common feature of earlier approaches is the neglect of correlations in the dynamics of the environment. In one approach [13], complete random lattice configurations are renewed with a constant renewal rate. In another, individual bonds are renewed independently of one another [12]. In our model, we have tried to incorporate correlations in the time development of the blocker from the start. The blocking periods account for the fact that, below p_c , the walker can be trapped longer than the average blocker hopping time τ because of the finite size of all clusters. In the pure renewal approach the walker is always started

again on a typical cluster at the time of the next renewal. Our approach allows the use of probabilistic arguments to arrive at a more detailed model of the blocker motion encapsulated in the density ψ_1 . This constitutes the main difference between our work and previous work. In addition, in our model, the typical renewal time, τ_r , depends on the blocker concentration, while it has been assumed to be constant before.

In summary, we have analyzed the dynamic percolation problem posed by ion transport in $\text{Ba}^{2+}-\text{Na}^+-\beta$ -alumina. The problem has been formulated in terms of continuous time random walks, using the case of frozen percolation as a starting point. For concentrations below the percolation threshold we predict a clear signature from the second time scale, the blocker hopping time τ . An even richer behaviour for $\sigma(\omega)$ is expected for situations with a sequential deblocking mechanism. The applicability of our model is not limited to solid electrolytes. Dynamic percolation models have recently been invoked to describe the conductivity of water in oil microemulsions [21]. Possible other applications include polymer electrolytes or transport through biomembranes [13].

We have presented an approximate solution for time (frequency) dependent response under conditions of dynamic percolation. Though we have carried out a calculation for the electrical conductivity, our approach is in fact considerably more general, and may apply to optical excitation transfer situations under dynamic conditions. The crossover in $\sigma(\omega)$ we have calculated for electrical transport translates to a "flattening off" of the mean-square displacement roughly at the time for geometrical rearrangement of the surroundings (here, the blocking ion hopping time). This should affect excitation diffusion, and may be observable in experiments which measure optical excitation dynamics. Our precise model would be relevant to structures where one random component blocks a second (carrier) component. Finite concentrations of the former create a percolation network for the latter. When the blockers are allowed to move in time, the network seen by the carriers changes with time, allowing for long range transport even if the instantaneous carrier site availability is less than p_c , the critical percolation concentration. Our methods should be sufficient for calculation of the corresponding expected optical excitation effect.

Acknowledgement

This research was supported in part by the US Office of Naval Research, and the Deutsche Forschungsgemeinschaft.

References

- [1] T. Holstein, S.K. Lyo and R. Orbach, in: Topics in applied physics, Vol. 49. Laser spectroscopy of solids, eds. W.M. Yen and P.M. Selzer, 2nd Ed. (Springer, Berlin, 1986) p. 39; H. Böttger and V.V. Bryksin, Hopping conduction in solids (Akademie Verlag, Berlin, 1985).
- [2] S. Chandra, Superionic solids (North-Holland, Amsterdam, 1981).
- [3] B. Dunn, R.M. Ostrom, R. SeEVERS and G.C. Farrington, Solid State Ionics 5 (1981) 203.
- [4] G.C. Farrington and B. Dunn, Solid State Ionics 7 (1982) 267.
- [5] R. SeEVERS, J. de Nuzzio, G.C. Farrington and B. Dunn, J. Solid State Chem. 50 (1983) 146.
- [6] J.P. Boilot, C. Collin, Ph. Colombari and R. Comes, Phys. Rev. B 22 (1980) 5912.
- [7] D. Stauffer, Introduction to percolation theory (Taylor and Francis, London, 1985).
- [8] B. Dunn and M. Underweiser, unpublished results.
- [9] R. Hilfer and R. Orbach, to be published.
- [10] T. Odagaki and M. Lax, Phys. Rev. B 24 (1981) 5284; I. Webman, Phys. Rev. Letters 47 (1981) 1496; S. Summerfield, Solid State Commun. 39 (1981) 401.
- [11] M. Sahimi, B.D. Hughes, L.E. Scriven and H.T. Davis, J. Chem. Phys. 78 (1983) 6849.
- [12] A.K. Harrison and R. Zwanzig, Phys. Rev. A 32 (1985) 1072.
- [13] S.D. Druger, M.A. Ratner and A. Nitzan, Phys. Rev. B 31 (1985) 3939.
- [14] J.C. Kimball and L.W. Adams, Phys. Rev. B 18 (1978) 5851.
- [15] J. Klafter and R. Silbey, Phys. Rev. Letters 44 (1980) 55.
- [16] J. Klafter, A. Blumen and M. Shlesinger, Phys. Rev. A 35 (1987) 3081.
- [17] H. Scher and M. Lax, Phys. Rev. B 7 (1973) 4491.
- [18] A. Blumen, J. Klafter and R. Silbey, J. Chem. Phys. 72 (1980) 5320.
- [19] J.W. Haus and K.W. Kehr, Phys. Rept. 150 (1987) 263.
- [20] W. Feller, An introduction to probability theory, Vol. 2 (Wiley, New York, 1971).
- [21] G.S. Grest, I. Webman, S.A. Safran and A.L.R. Bug, Phys. Rev. A 33 (1986) 2842.